Article type: SPECIAL ISSUE ARTICLE

Title: **Recent progress on the flight of dragonflies and damselflies**

Authors: Toshiyuki Nakata[1,2], Per Henningsson[3], Huai-Ti Lin[4] and Richard J. Bomphrey[1]

Affiliation:

1 Structure and Motion Laboratory, Department of Comparative Biomedical Sciences, Royal Veterinary College, North Mymms, Hatfield AL9 7TA, UK

2 Graduate School of Engineering, Chiba University, 1-33, Yayoi-cho, Inage-ku, Chiba-shi, Chiba 263-8522, Japan

3 Department of Biology, Lund University, Ecology Building, 223 62 Lund, Sweden

4 Department of Bioengineering, Imperial College London

Correspondence details:

Richard J. Bomphrey

e-mail: rbomphrey@rvc.ac.uk

Acknowledgements:

This work was partly supported by JSPS KAKENHI (JP18H05468) to T.N, Swedish research council (2013-4838 and 2018-04292) to P.H., Biotechnology and Biological Sciences Research Council (BB/R002509/1) to H.T.L and (BB/R002657/1) to R.J.B.

Abstract

Remarkable flight performance is key to the survival of adult Odonata. They integrate varied three-dimensional architectures and kinematics of the wings, unsteady aerodynamics, and sensory feedback control in order to achieve agile flight. Therefore, a diverse range of approaches are necessary to understand their flight strategy comprehensively. Recently, Bomphrey *et al.* (2016) have presented new data in several key areas in Odonata such as measurement of surface topographies, computational fluid dynamic analyses, quantitative flow visualization using particle image velocimetry, and optical tracking of free flight trajectories in laboratory environments. In this paper, we briefly review those findings alongside more recent studies that have advanced our understanding of the flight mechanics of Odonata still further.

Keywords

Odonata; dragonfly; damselfly; biomechanics; flight; aerodynamics; visual control

Introduction

Flight performance of Odonata greatly affects their survivorship because it directly influences darting hunts, hawking flights, prey selection, interception and capture, predator evasion, and fuel economy during short commutes or long migration journeys. The flight of Odonata, including gliding, hovering, and manoeuvring modes, is achieved by tuning the aerodynamic forces acting on their wings through the control of wing kinematics on the basis of input from multiple sensors. Various architectural components in Odonata wings passively prescribe the posture and shape of the wings. Kinematics of their fore and hind wings in concert with three-dimensional wing geometries determine aerodynamic performance through the interaction between the wings and the surrounding air. Sensory inputs are monitored to coordinate the motor activities for routine flight control and specialist behavioural modes such as prey capture and conspecific pursuit. Considerable parts of the overall strategy for efficient and robust flight are still unknown because of the multiscale complexities of interactions between morphology, aerodynamics, sensory integration, and motor control.

Toward a comprehensive understanding of the strategy of Odonata, Bomphrey, Nakata, Henningsson, and Lin (2016) have recently presented a wide-ranging description of the biomechanical and neurophysiological aspects of flight alongside new results acquired using a broad suite of modern methods. In this paper, we have briefly summarised the results on the state-of-the-art with some additional updates from more recent studies.

Structural dynamics of the odonatan wing

The wings of the Odonata are hierarchical structures. Recent research progress, especially those employing computational approaches, have revealed the function of many structural

elements. Wing deformation is controlled passively through interactions of the detailed structural elements in the wings. Key elements, including the longitudinal veins, cross-veins, vein-joints (often including flexible resilin sections), the basal complex (defined here as the three-dimensional structure of proximal part of the wing), nodus, and membrane (Rajabi et al., 2016), are particularly important, since the dynamically deforming wing shapes directly affect aerodynamic performance (Young, Walker, Bomphrey, Taylor, & Thomas, 2009). Computational structural dynamic (CSD) analyses on odonatan wings suggest that specific geometries of the vein-joints (Rajabi, Ghoroubi, Darvizeh, Appel, & Gorb, 2016) or the nodus (Rajabi, Ghoroubi, Stamm, Appel, & Gorb, 2017) are responsible for the dorsoventral asymmetry of the wing deformation. While these elements function to control the wing deformation under aerodynamic loads passively during flight, collision with obstacles may lead to excessive loading and structural damage. The rubber-like protein, resilin, present at some vein-joints can considerably reduce the stress concentration in joints when the wings are deformed (Rajabi, Shafiei, Darvizeh, & Gorb, 2016), which may help to mitigate effects of collisions (Mountcastle, Helbling, & Wood, 2019). This is likely to be a secondary function of resilin, following a principal role in facilitating elastic wing deformation during normal flight.

Aerodynamics of gliding and flapping flight

In addition to the wing deformation controlled passively through fluid-structure interactions and inertial bending, the three-dimensional shape and arrangement of the four wings are also important for the flight performance of Odonata. Bomphrey *et al.* (2016) have performed computational fluid dynamic (CFD) analyses of gliding flight using a low Reynolds number aerodynamic simulator (Liu, 2009) with specific focus on the effect of the

85 corrugated chordwise cross section and the interaction between fore and hind wings in
86 gliding.
87 The three-dimensional wing geometries required for this analysis were reconstructed by
88 photographing a series of cross sections illuminated by a laser line projection (figure 1a). By
89 using the resulting surface topology for CFD analysis, it was found that natural-scale
90 corrugation does not give rise to a dramatic decrease in the lift-to-drag ratio that was
91 observed for corrugations amplitudes that were exaggerated, and larger than those found in
92 nature (figure 1b,c). Therefore, corrugations can substantially increase wing stiffness
93 without greatly increasing material volume and, moreover, the corrugated structure does
94 not substantially increase aerodynamic costs.
95 The fore- and hindwing interactions are investigated further by using CFD analyses with the
96 angle of attack, sweep and dihedral angles of the wings relative to the body measured from
97 field photography (figure 1d). The fore and hind wings are highly efficient relative to other
98 insect fliers because of their high aspect ratios. By comparing the aerodynamic performance
99 of gliding with fore and hind wings in tandem against a baseline of fore and hind wings
100 acting in isolation – i.e. without aerodynamic interactions – Bomphrey *et al.* (2016)
101 discovered that the dragonflies keep the performance of each wing high by trimming the
102 wing angles to glide efficiently (figure 1e-f).
103 In conventional, fixed-wing aircraft, high aspect ratio wings achieve better lift-to-drag ratios
104 than less-slender alternatives. This typically comes at the cost of manoeuvrability because
105 the wing's moment of inertia is increased. However, it is worth noting that this relationship
106 is not always maintained in insects. In genetically modified fruit flies, lines with higher
107 aspect ratio wings showed enhanced manoeuvrability, albeit at the cost of a higher power
108 requirement (Ray, Nakata, Henningsson, & Bomphrey, 2016). Odonata overcome this

physical trade-off of efficiency versus manoeuvrability by operating their four wings independently. For example, damselflies achieve yaw turn by the control of the angle of attack of each wing as well as the flapping velocities of the wings (Zeyghami, Bode-Oke, & Dong, 2017). Their backward flight is enabled by force vectoring, which is based on tilting the stroke plane to adjust the direction of the net aerodynamic forces (Bode-Oke, Zyghami, & Dong, 2018). Abdominal deflection increases the yaw velocity by reducing the moment of inertia and thus the flight torque required for the manoeuvre (Bode-Oke, Zeyghami, & Dong, 2017b). During take-off, which requires large and finely-tuned aerodynamic forces to accelerate in a desired direction, damselflies generate aerodynamic forces that reach three-times body weight, operating each of the four wings at high angles of attack (Bode-Oke, Zeyghami, & Dong, 2017a). Similarly, dragonflies utilise high angles of attack and the synchronous flapping of fore and hind wings to generate large vertical forces at the beginning of take-off, later switching to lower angles of attack and counter-stroking (out-of-phase) flapping to generate large thrust (Alexander, 1984; Li, Zheng, Pan, & Su, 2018; Thomas, Taylor, Srygley, Nudds, & Bomphrey, 2004). The orientation of aerodynamic forces after the take-off are controlled by adjusting the ratio of downstroke to upstroke duration and the angle of attack of the wings (Shumway, Gabryszuk, & Laurence, 2018).

To support their weight when flapping, the Odonata rely heavily on unsteady aerodynamic mechanisms. In common with many insects, they use a separated flow pattern that delays aerodynamic stall and allows the wing to operate, momentarily, at angles of attack above the steady condition stall angle. During this moment of delayed stall, flow separates from the surface at the leading edge but subsequently re-attaches further back along the chord, ultimately leaving the trailing edge smoothly and satisfying a requirement for the flow on upper and lower surfaces to meet at the sharp trailing edge, known as the Kutta condition.

Inside the separation bubble (the volume bounded by the point at which flow detaches and reattaches on the chord), the flow rolls up into a swirling, leading-edge vortex (LEV), allowing the wing to operate at high angles of attack producing remarkably high lift. Quantitative flow visualizations using a laser-based technique called particle image velocimetry (PIV), where the air is seeded with tiny droplets of olive oil, confirmed the qualitative descriptions of the flow topology shown by Bomphrey *et al.* (2002) and described in detail by Thomas *et al.* (2004) (figure 2a). The typical, counter-stroking, kinematic pattern leads to a cylindrical LEV spanning the thorax (figure 2b) from forewing tip to forewing tip (figure 2c), while the hindwing exhibits conventional attached flow. Using their quantitative PIV data, from *Sympetrum striolatum* and *Aeshna mixta*, Bomphrey *et al.* (2016) have further discovered that: 1) the core diameter of the leading-edge vortex is substantially greater than the mean chord length of the forewings at all spanwise positions from the centreline to the wing tips; 2) the diameter and circulation increase from root to tip in *A. mixta*; 3) the spanwise contribution to weight support increases from root to tip in both species; and 4) axial velocities at the core of the leading-edge vortex can be quite strong in either direction (at least during slow forward flight), and is not, therefore, an essential prerequisite of vortex stability during the period of a single half stroke as has been suggested for other insects (Birch & Dickinson, 2001). A recent flow visualization study by Hefler *et al.* (2018) also confirmed the existence of the LEV on the hind wings during free flight, suggesting its dynamics are under the effect of the aerodynamic interactions between fore and hind wings.

Bomphrey *et al.* (2016) have also used quantitative flow measurements to estimate the efficiency with which lift is generated. Span efficiency (e_i) is the ratio of the power required to generate lift under ideal aerodynamic loading conditions on the wing to the power

157 required in reality: the ideal power divided by the induced power. Since the power required
158 to generate a given lift is derived from the induced flow velocity, span efficiency can be
159 measured empirically as the deviation of the downwash velocity profile behind the wings
160 from the theoretical ideal of an even distribution across the span. In the case of a fixed
161 wing, an elliptical planform gives the highest span efficiency by generating an even
162 downwash distribution across the span. Because the velocity of flapping wings increases
163 linearly with distance from the wing hinge, flapping wings will deviate from an elliptical plan
164 form and maximise their efficiency if the wing is broad at the root and tapers towards the
165 tip. The tapering should compensate for the wing's velocity distribution. If we ignore wing
166 twist, or assume that it is comparable across the Odonata, the Anisoptera are, therefore,
167 predicted to perform better than the Zygoptera, since anisopterans have wing shapes with
168 chord lengths that taper toward the wing tip, while zygopterans have wing chord lengths
169 that lengthen towards the wing tip. We tested this prediction by estimating the span
170 efficiencies for 24 individuals of six Odonata species in free flight in a custom-built wind
171 tunnel, following the protocol of Henningsson and Bomphrey (2013). Figure 2d shows a time
172 series of transects through the downwash at 1 millisecond intervals for representative
173 examples of *Enallagma cyathigerum*. The colour and relief show the magnitude of the
174 downwash velocity behind the trailing edges of the hind wings, black solid and dashed lines
175 show the vertical excursion of the undulating left and right hindwing tip vortices throughout
176 the sequence. Ensemble-averaged temporal variations in span efficiencies are shown in
177 figure 2e. As predicted from the difference in the wing shape (Bomphrey, et al., 2016), the
178 Zygoptera with narrower wing base have lower span efficiencies (figure 2e) and span
179 efficiency is strongly correlated with taper ratio (figure 2f), confirming the relationship
180 between wing planform and aerodynamic efficiency during flapping flight. At the cost of

lowered efficiency, the Zygopteran planform shifts the wing's centre of pressure away from the insect's centre of mass, which increases the distance swept by the distal area of the wing. This evolutionary solution might expand the kinematic envelope available and increase the torque that can be generated at the wing hinge when manoeuvring.

Flight performance

Bomphrey *et al.* (2016) presented two sets of data on the flight performance of Odonata, aiming at providing standardized baseline data and showing quantitative differences in flight performance during cruising, predatory and territorial escort flights. As an example, figure 3a-c shows the total speed, centripetal acceleration and turn rate of nine species of Odonata in a flight arena, acquired using calibrated stereo-cameras (following the protocol detailed previously (Henningsson & Bomphrey, 2013; Ray, et al., 2016)). Statistical analyses suggested that: 1) the Zygoptera tended to fly more slowly than the Anisoptera, but the majority of species preferred to fly at between 1 and 2 m s^{-1}; 2) the centripetal accelerations were relatively modest, with only *Sympetrum sanguineum* frequently accelerating over 3g when cornering; 3) turn rates can reach up to 1000 deg s^{-1} in several species. Another set of the probability density function in figure 3d-f shows the speed, turn rate and turn radius of *Plathemus lydia* during cruising, predatory and territorial flights, recorded using the protocol described by Mischiati *et al.* (2015). It is clear that the predatory and territorial flights are more demanding than cruising flight; territorial flight and prey interception flight exhibited higher speeds more frequently (figure 3d) and also more rapid turns (figure 3e). Territorial flights in our experimental observations were faster than the predatory flights, but the turn radius of the predatory flights was slightly tighter than those observed during territorial flights (figure 3f). We do not expect these behaviours to exhibit the full repertoire of each

205 species, but the standardization within our well-defined and repeatable settings is useful for
206 benchmarking a conservative flight performance envelope. The metrics provided in this
207 study highlight coarse interspecies variability for future investigations into comparative
208 flight performance.
209
210 **Neurophysiology of dragonfly vision**
211 The dragonfly's impressive visual abilities have motivated numerous studies on the
212 neurophysiology of small target detections. The most notable ones can be dated back to the
213 1980's with the discovery of the target selective descending neurons (TSDNs) that transmit
214 target movement information from the visual centre in the head to the motor centre in the
215 thorax (Olberg, 1986). Later, the small target motion detectors (STMDs) were discovered in
216 the third visual neuropil, lobula (O'Carroll, 1993). Both classes of neurons respond to small
217 shadows moving in a relatively wide area of the visual field. TSDNs were assumed to be the
218 downstream neurons of STMDs for a long time, yet a direct evidence has never been
219 established. On-going work attempts to establish the functional role of TSDNs and the signal
220 transformation from the visual system.
221 Behavioural studies and physiological studies go hand-in-hand to advance our
222 understanding of dragonfly vision. Through precise measurement of dragonfly head
223 movement during repeated prey interception flights, Mischiati *et al.* (2015) established the
224 predictive nature of dragonfly prey interception behaviour. While the target interception
225 trajectory can be achieved via a fast reactive control mechanism, the way the dragonfly's
226 head cancels expected target movement demonstrates the role of predictive control. This
227 observation was reinforced by the discovery of a strong predictive neural facilitation in
228 STMDs (Wiederman, Fabian, Dunbier, & O'Carroll, 2017). As the target moves across the

receptive field of a STMD neuron, the sensitivity of target detection in front of the current target position is enhanced by over 50%. This demonstrates that the visual system indeed has information about the expected future target location. From scrutinizing visual parameters of the dragonfly's prey selection, we have shown that target selection is highly tuned to the interception flight dynamics (Lin & Leonardo, 2017). This selection might be correlated but not purely driven by target detection limits. Dragonflies have incredible sensitivity to detecting targets that are smaller than single photoreceptor. A recent study compared the photoreceptor sensitivity to small targets in dragonflies, hoverflies, honey bee drones, and blowflies (Rigosi, Wiederman, & O'Carroll, 2017). The result confirmed a similar subpixel target detection level (<0.2° target) as reported by the target selection behaviour study (Lin & Leonardo, 2017).

Finally, a recent study compared visual motion detection responses in dragonflies and macaque monkeys (Nitzany et al., 2017). It shows that both systems respond to some motion cues that cannot be explained by the classic Hassenstein-Reichardt model. With the discovery of a class of wide-field sensitive neurons in the dragonfly lobula (Evans, O'Carroll, Fabian, & Wiederman, 2018), we expect dragonflies to serve as an alternative model system for understanding the fundamental mechanism of motion detection.

Concluding remarks

We have briefly reviewed the current state-of-the-art of research on the biomechanics of odonatan flight. The use of computational structural and fluid dynamic analysis has separately driven progress toward a more complete understanding of the functional morphology of the wings of the Odonata and their flight mechanics. Computational analyses revealed that wing deformation is passively controlled by the hierarchical architecture of

253 odonatan wings, but its effect on flight performance is yet to be resolved. This is because
254 the coupling of passive wing deformation and unsteady aerodynamics is not yet taken into
255 account. Nor is it well understood how the steering muscles modify wing shape during
256 cyclical flapping or manoeuvres. Wing deformations affect the sensory encoding of
257 mechanosensors mounted on the veins but we do not yet know how wing shape changes
258 are monitored by the flight controller. It is also not yet clear how body rotations affect wing
259 deformations and, thus, how those deviations from the encoding expected during straight
260 and manoeuvring flight could be used in flight control in turbulent atmospheric conditions.
261 This sensory role of the wings in stabilisation has not been shown in dragonflies although
262 there is a growing body of work in the context of moth wings acting as gyroscopic sensors
263 (Pratt, Deora, Mohren, & Daniel, 2017) analogous to the well-studied function of halteres in
264 Diptera. Therefore, we must work towards a comprehensive wing structural model coupled
265 with the surrounding fluid dynamics. With this model we can begin to understand the
266 functional significance of each structural element and also to characterize the role of wing
267 mechanosensors in flight control. Current advances in computational modelling methods
268 certainly help towards this comprehensive fluid-structure interaction analysis. Aerodynamic
269 experiments on real animals, where wing surfaces and flow velocities close to the wings can
270 be measured simultaneously, are now possible and will be vital for computational model
271 validation (Nila et al., 2016). The combination of such empirical and computational
272 approaches would add strength and robustness to the results.
273 Several more key areas that will advance our understanding of the flight strategy of the
274 Odonata were identified by Bomphrey *et al.* (2016). The behavioural repertoire of the
275 Odonata is diverse, and we must develop new approaches that allow high throughput, high-
276 quality wing kinematics measurements (Koehler, Liang, Gaston, Wan, & Dong, 2012; Walker,

Thomas, & Taylor, 2009). The use of artificial targets with prescribed perturbation will allow us to formulate behavioural models by artificially eliciting predictable and repeatable flight responses (Fabian, Sumner, Wardill, Rossoni, & Gonzalez-Bellido, 2018; Mischiati, et al., 2015). The wings are, of course, driven by the flight motor and wing hinge; in order to understand the interplay of these musculoskeletal elements during the various behaviours, a combination of tethered flight and wireless recording of the flight muscles would be very useful.

Comprehensive analyses are extremely challenging, but flight in Odonata represents a fine example of a natural aerial system in which complex wing morphology, unsteady aerodynamics and neural feedback control are integrated to achieve extraordinary flight behaviour. On-going work focuses on revealing the neural representation of wing aeroelasticity. Understanding such a system can inspire the development of novel agile micro aerial vehicles with sophisticated 'fly-by-feel' control systems that use mechanosensory information about loads on the wing surface in the flight controller. Finally, while behavioural and neurophysiological studies continue to work synergistically to advance our understanding of flight control, we believe it is necessary to retain biomechanics as a fundamental link between the two, to set each in context, and to answer the proximate questions of flight in the Odonata and other insects.

References

Alexander, D. E. (1984). Unusual phase relationships between the forewings and hindwings in flying dragonflies. *Journal of Experimental Biology, 109*, pp. 379-383.

Birch, J. M., & Dickinson, M. H. (2001). Spanwise flow and the attachment of the leading-edge vortex on insect wings. *Nature, 412*, pp. 729-733.

Bode-Oke, A. T., Zeyghami, S., & Dong, H. (2017a). Aerodynamics and flow features of a damselfly in takeoff flight. *Bioinspiration & Biomimetics, 12*(5), p 056006.

Bode-Oke, A. T., Zeyghami, S., & Dong, H. (2017b). Optimized Body Deformation in Dragonfly Maneuvers. *arXiv*, p 1707.07704.

Bode-Oke, A. T., Zyghami, S., & Dong, H. (2018). Flying reverse: kinematics and aerodynamics of a dragonfly in backward free flight. *Journal of the Royal Society Interface, 15*, p 20180102.

Bomphrey, R. J., Nakata, T., Henningsson, P., & Lin, H. T. (2016). Flight of the dragonflies and damselflies. *Philosophical Transactions of the Royal Society B, 371*(1704), p 20150389.

Bomphrey, R. J., Srygley, R. B., Taylor, G. K., & Thomas, A. L. R. (2002). Visualising the flow around insect wings. *Physics of Fluids, 14*, p S4.

Evans, B. J., O'Carroll, D. C., Fabian, J. M., & Wiederman, S. D. (2018). Differential adaptation to visual motion allows robust encoding of optic flow in the dragonfly. *bioRxiv*, p 496588.

Fabian, S. T., Sumner, M. E., Wardill, T. J., Rossoni, S., & Gonzalez-Bellido, P. T. (2018). Interception by two predatory fly species is explained by a proportional navigation feedback controller. *Journal of the Royal Society Interface, 15*, p 20180466.

Hefler, C., Qui, H., & Shyy, W. (2018). Aerodynamic characteristics along the wing span of a dragonfly *Pantala flavescens*. *Journal of Experimental Biology, 221*, p jeb171199.

Henningsson, P., & Bomphrey, R. J. (2013). Span efficiency in hawkmoths. *Journal of the Royal Society Interface, 10*(84), p 20130099.

Koehler, C., Liang, Z., Gaston, Z., Wan, H., & Dong, H. (2012). 3D reconstruction and analysis of wing deformation in free-flying dragonflies. *Journal of Experimental Biology, 215*, pp. 3018-3027.

Li, Q., Zheng, M., Pan, T., & Su, G. (2018). Experimental and numerical investigation on dragonfly wing and body motion during voluntary take-off. *Scientific Reports, 8*, p 1011.

Lin, H. T., & Leonardo, A. (2017). Heuristic rules underlying dragonfly prey selection and interception. *Current Biology, 27*, pp. 1124-1137.

Liu, H. (2009). Integrated modeling of insect flight: from morphology, kinematics to aerodynamics. *Journal of Computational Physics, 228*, pp. 439-459.

Mischiati, M., Lin, H. T., Herold, P., Imler, E., Olberg, R., & Leonardo, A. (2015). Internal models direct dragonfly interception steering. *Nature, 517*(7534), pp. 333-338.

Mountcastle, A. M., Helbling, E. F., & Wood, R. J. (2019). An insect-inspired collapsible wing hinge dampens collision-induced body rotation rates in a microrobot. *Journal of the Royal Society Interface, 16*, p 20180618.

Nila, A., Phillips, N., Bomphrey, R. J., Bleischwitz, R., de Kat, R., & Ganapathisubramani, B. (2016) *Optical measurements of fluid-structure interactions for the description of nature-inspired wing dynamics*. Paper presented at the 2016 RAeS Applied Aerodynamics Conference, Bristol, UK.

Nitzany, E., Menda, G., Shamble, P. S., Golden, J. R., Hu, Q., Hoy, R. R., & Victor, J. (2017). Neural computations combine low-and high-order motion cues similarly, in dragonfly and monkey. *bioRxiv*, p 240101.

O'Carroll, D. (1993). Feature-detecting neurons in dragonflies. *Nature, 362*, p 541.

Olberg, R. M. (1986). Identified target-selective visual interneurons descending from the dragonfly brain. *Journal of Comparative Physiology A, 159*, pp. 827-840.

Pratt, B., Deora, T., Mohren, T., & Daniel, T. (2017). Neural evidence supports a dual sensory-motor role for insect wings. *Proceedings of the Royal Society B, 284*(1862), p 20170969.

Rajabi, H., Ghoroubi, N., Darvizeh, A., Appel, E., & Gorb, S. N. (2016). Effects of multiple vein microjoints on the mechanical behaviour of dragonfly wings: numerical modelling. *Royal Society Open Science, 3*, p 150610.

Rajabi, H., Ghoroubi, N., Stamm, K., Appel, E., & Gorb, S. N. (2017). Dragonfly wing nodus: A one-way hinge contributing to the asymmetric wing deformation. *Acta Biomaterialia, 60*, pp. 330-338.

Rajabi, H., Rezasefat, M., Darvizeh, A., Dirks, J.-H., Eshghi, S., Shafiei, A., Mirzababaie Mostofi, T., & Gorb, S.N. (2016). A comparative study of the effects of constructional elements on the mechanical behaviour of dragonfly wings. *Applied Physics A, 122*, p 19.

Rajabi, H., Shafiei, A., Darvizeh, A., & Gorb, S. N. (2016). Resilin microjoints: a smart design strategy to avoid failure in dragonfly wings. *Scientific Reports, 6*, p 39039.

Ray, R. P., Nakata, T., Henningsson, P., & Bomphrey, R. J. (2016). Enhanced flight performance by genetic manipulation of wing shape in *Drosophila*. *Nature Communications, 7*, p 10851.

Rigosi, E., Wiederman, S. D., & O'Carroll, D. C. (2017). Photoreceptor signalling is sufficient to explain the detectability threshold of insect aerial pursuers. *Journal of Experimental Biology, 220*, pp. 4364-4369.

Shumway, N. M., Gabryszuk, M., & Laurence, S. J. (2018) *Flapping tandem-wing aerodynamics: dragonflies in steady forward flight*. Paper presented at the 2018 AIAA Aerospace Sciences Meeting, Florida.

Thomas, A. L. R., Taylor, G. K., Srygley, R. B., Nudds, R. L., & Bomphrey, R. J. (2004). Dragonfly flight: free-flight and tethered flow visualizations reveal a diverse array of unsteady lift-generating mechanisms, controlled primarily *via* angle of attack. *Journal of Experimental Biology, 207*, pp. 4299-4323.

Walker, S. M., Thomas, A. L. R., & Taylor, G. K. (2009). Photogrammetric reconstruction of high-resolution surface topographies and deformable wing kinematics of tethered locusts and free-flying hoverflies. *Journal of the Royal Society Interface, 6*, pp. 351-366.

Wiederman, S. D., Fabian, J. M., Dunbier, J. R., & O'Carroll, D. C. (2017). A predictive focus of gain modulation encodes target trajectories in insect vision. *eLife, 6*, p e26478.

Young, J., Walker, S. M., Bomphrey, R. J., Taylor, G. K., & Thomas, A. L. R. (2009). Details of insect wing design and deformation enhance aerodynamic function and flight efficiency. *Science, 325*, pp. 1549-1552.

Zeyghami, S., Bode-Oke, A. T., & Dong, H. (2017). Quantification of wing and body kinematics in connection to torque generation during damselfly yaw turn. *Science China Physics, Mechanics & Astronomy, 60*(1), p 014711.

Figures

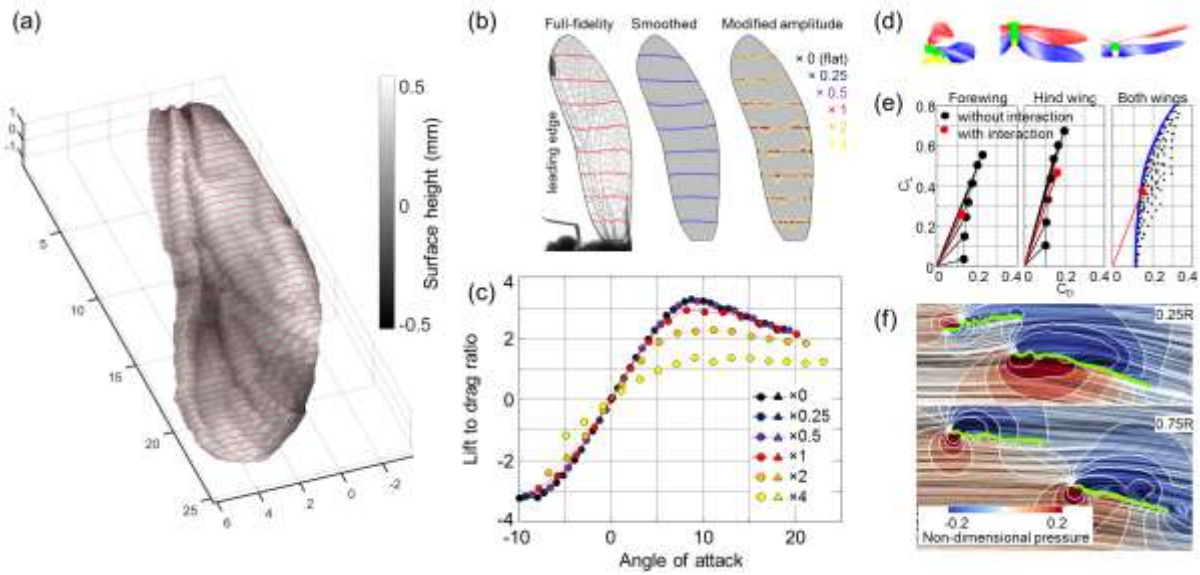

Figure 1. Three-dimensional surface geometry and gliding aerodynamics of dragonfly wings. (a) The complex three-dimensional geometry of the wings for CFD analysis. (b) Selected cross sections of the full-fidelity wing, smoothed wing and the wings with modified amplitude. (c) The lift-to-drag ratio for the exaggerated and reduced corrugation models. (d) Three-dimensional models of the forewing (red), hindwing (blue) and the upper (green) and lower (yellow) surfaces of the thorax. (e) Lift and drag coefficient polars of the fore and hind wings with (red) or without (black) aerodynamic interactions. (e) The two-dimensional flow structure shown by line integral convolution (LIC) streamlines and pressure distribution contours around the fore and hind wings at 25% and 75% of wing length. The positive and negative pressure regions of each wing connect with each other, revealing an aerodynamic interaction between the ipsilateral wing pairs. This figure is reproduced from Bomphrey *et al.* (2016).

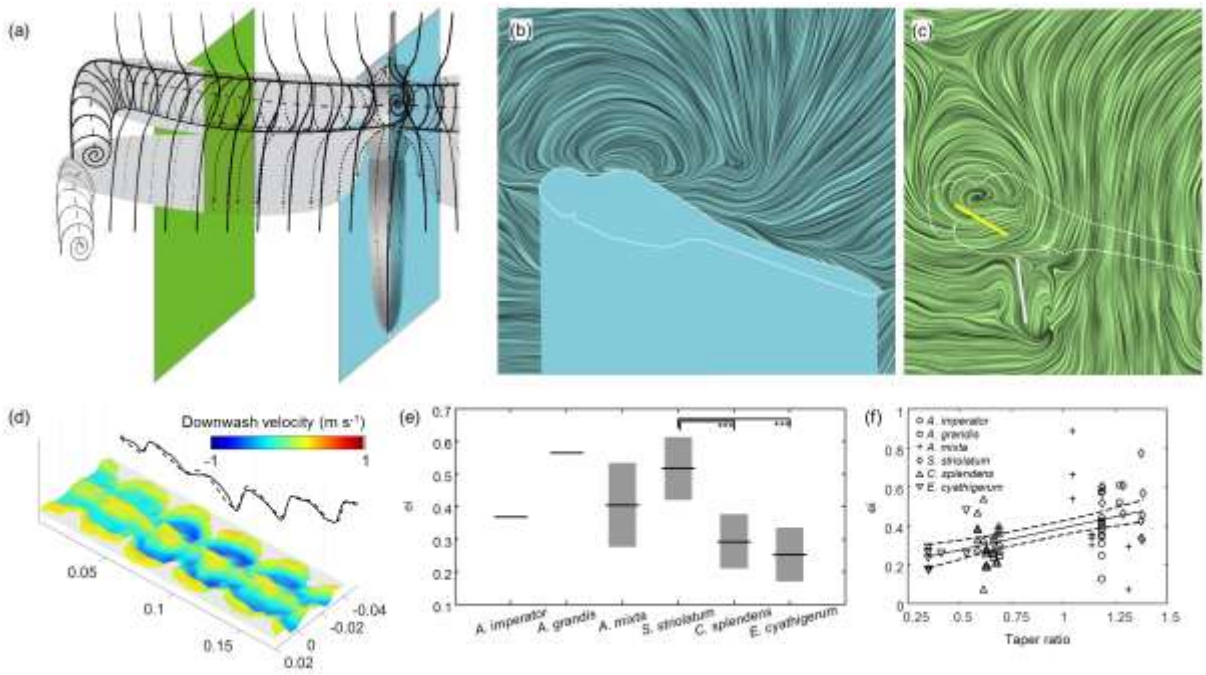

396

397

398 Figure 2. Figure 2 Flapping wing aerodynamics of Odonata. (a) Topology of the leading-
399 edge vortex of a dragonfly. Cross section of the flow at (b) the centreline of the body and (c)
400 approximately 45% of the wing's length from hinge to tip measured by PIV, with
401 instantaneous streamlines visualized by LIC. (d) Example sequence of the time-resolved
402 induced downwash of *Enallagma cyathigerum*. Both the relief and colour represent
403 downwash velocity, with shades in blue/cyan representing downward velocities
404 corresponding to positive lift and shades in red/yellow upward velocities corresponding to
405 negative lift. (e) The span efficiency of each species. Boxes show median values with 95%
406 confidence intervals. Post hoc pairwise ANOVA under a/the Tukey criterion shows the
407 differences between *Sympetrum striolatum* and two of the Zygoptera are significant ($p <$
408 0.001). (f) The taper ratio is positively correlated with span efficiency ($p < 0.001$, $R^2 = 0.24$).
409 Solid and dashed lines show the least-squares regression slope with 95% confidence
410 intervals. This figure is reproduced from Bomphrey *et al.* (2016).

411

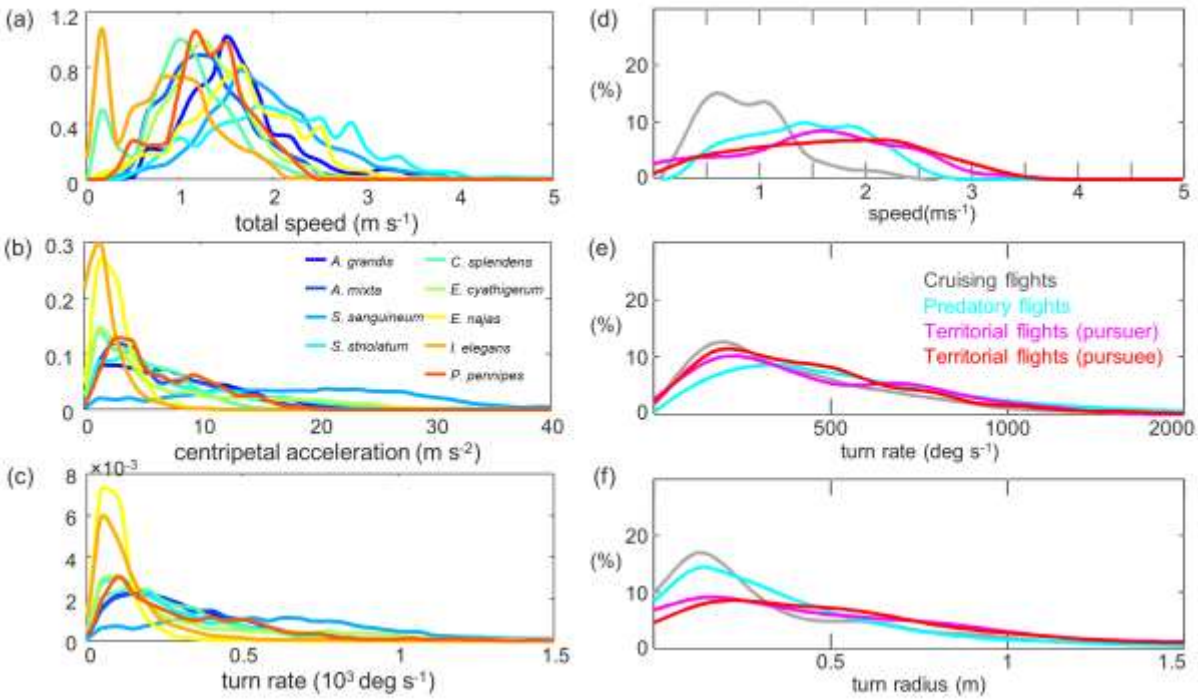

412

413

414 Figure 3. Flight performance of Odonata. (a) Total speed, (b) centripetal acceleration, and

415 (c) turn rate of nine species of Odonata. (d) Speed, (e) turn rate and (f) turn radius of

416 *Plathemus Lydia* during cruising, hunting and territorial flights. This figure is reproduced

417 from Bomphrey *et al.* (2016).